THE JOURNAL OF PHYSICAL CHEMISTRY B

Article

pubs.acs.org/JPCB

Comparison of PELDOR and RIDME for Distance Measurements between Nitroxides and Low-Spin Fe(III) Ions

Dinar Abdullin, Fraser Duthie, Andreas Meyer, Elisa S. Müller, Gregor Hagelueken, and Olav Schiemann*

Institute of Physical and Theoretical Chemistry, University of Bonn, Wegelerstrasse 12, 53115 Bonn, Germany

Supporting Information

ABSTRACT: EPR-based nanometre distance measurements are becoming ever more important in structural biology. Usually the distance constraints are measured between two nitroxide spin labels. Yet, distance measurements between a metal center and spin labels enable, e.g., the localization of metal ions within the tertiary fold of biomolecules. Therefore, it is important to find methods that provide such distance information quickly, with high precision and reliability. In the present study, two methods, pulsed electron−electron double resonance (PELDOR) and relaxation-induced dipolar modulation enhancement (RIDME), are compared on the heme-containing and spin-labeled cytochrome P450cam. Special emphasis is put on the optimization of the dead-time free RIDME experiment and several ways of data analysis. It turned out that RIDME appears to be better suited for distance measurements involving metal ions like low-spin Fe^{3+} than PELDOR.

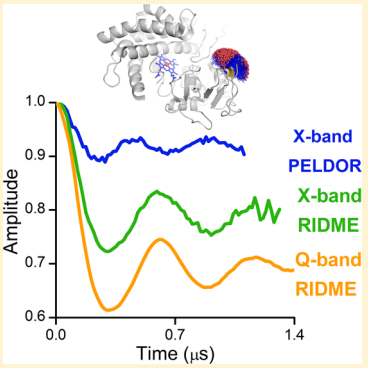

INTRODUCTION

Distance measurements by pulsed electron paramagnetic resonance (EPR) provide valuable information about the structure and dynamics of proteins and oligonucleotides.[1−3] The most commonly used technique is pulsed electron−electron double resonance (PELDOR).[4,5] It is often applied to measure the distance between two nitroxide spin labels site-specifically attached to a biomolecule.[2] In addition to nitroxides, there is a keen interest of using naturally occurring paramagnetic cofactors, like metal ions,[6−8] amino acids[9,10] or flavins,[11,12] for such distance measurements. In this way, new applications like the localization of metal ions within the fold of metalloproteins become possible.[13] So far, the majority of reported PELDOR studies on metal centers are dealing with low-spin Cu^{2+} ions,[6−8] iron−sulfur clusters[14,15] or manganese clusters.[16] Besides them, Gd^{3+} ions are often used as artificially introduced spin labels for PELDOR measurements.[17,18] All these centers usually display a moderate *g*-factor anisotropy and relatively long relaxation times. In contrast, PELDOR experiments involving metal ions, like Fe^{3+} or Mn^{2+}, are limited to a few recent reports.[19−22] This may stem from the fact that PELDOR measurements on such metal ions are usually time-consuming and demanding to analyze due to short relaxation times, low signal-to-noise ratio (SNR) and orientation selectivity. Furthermore, spin couples that consist of a nitroxide spin label and a metal center with largely different *g*-values than the nitroxide are difficult to study with the double-frequency PELDOR technique, due to the limited bandwidths of EPR resonators and microwave amplifiers. In this case, the use of single-frequency EPR techniques could be advantageous. One possibility, used already early on, would be to study how the relaxation of a slowly relaxing spin center, e.g., a nitroxide, changes due to the dipolar coupling to a faster relaxing spin center, e.g., a metal ion.[23] However, the extraction of distances by this relaxation method has a significant complexity that stems from the fact that the dipolar coupling leads only to an additional exponential decay of the signal and not to an oscillation and it needs the reference measurement without the metal center. In contrast, another single-frequency technique called relaxation-induced dipolar modulation enhancement (RIDME)[24] has been shown to yield time traces in which the dipolar coupling manifests itself as an oscillation of the signal. Therefore, we set up to compare RIDME and PELDOR, when applied to the spin couple low-spin Fe(III)/nitroxide. The advantage of the RIDME experiment being that the metal ion spin is flipped by spontaneous relaxation rather than by a microwave pulse as it is in PELDOR.

Since the pioneering work of Kulik et al.,[24] the RIDME experiment has been significantly advanced. The disadvantage of the original three-pulse RIDME sequence is its dead time, which obscures the initial part of the signal and, therefore, complicates the extraction of the distance distribution. Introduction of the four-pulse sequence allowed one to reduce the dead time,[25] and the five-pulse sequence recently proposed by the lab of Huber has been shown to be dead time free.[26] Although the three and four-pulse versions of RIDME were applied to a wide range of spin systems,[27−32] the use of the new dead-time free RIDME accounts only for a few studies on nitroxide/nitroxide and Gd^{3+}/Gd^{3+} model systems,[26,33] and on the Fe^{3+}−nitroxide spin couple in cytochrome *f*.[26] Note that the

Special Issue: Wolfgang Lubitz Festschrift

Received: March 4, 2015
Revised: May 20, 2015

DOI: 10.1021/acs.jpcb.5b02118
J. Phys. Chem. B XXXX, XXX, XXX−XXX

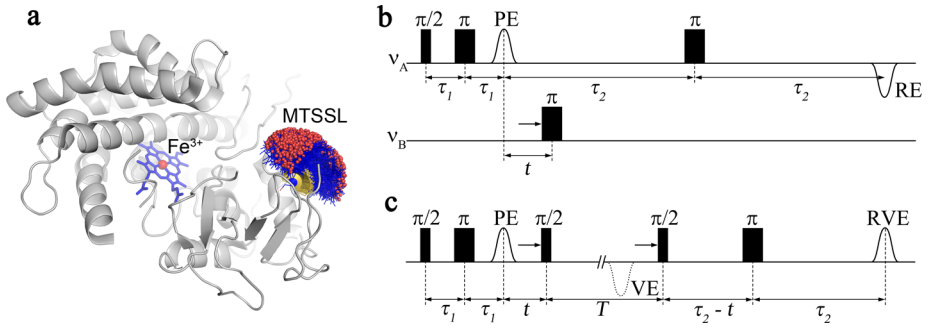

Figure 1. (a) Model of MTSSL-labeled cytochrome P450cam mutant C58R$_1$ created by means of the program mtsslWizard[35,36] using the crystal structure of the native form of the protein (PDB 3L61). The Fe^{3+}-MTSSL distances were measured using (b) the PELDOR and (c) the five-pulse RIDME experiments. The positions of the primary (PE), virtual (VE), refocused (RE), and refocused virtual (RVE) echoes are marked in the pulse sequences.

RIDME signals reported for the Fe^{3+}−nitroxide spin couple were shorter than 1 μs and showed no modulation, leaving the question of precise distance measurements for the Fe^{3+} spin center open. Another important aspect of the RIDME experiment concerns the removal of spin echo envelope modulations (ESEEM)[34] from the original signal. To do this, several approaches were introduced but have not been compared to each other.[26−29]

Therefore, we compare here PELDOR and the dead-time free RIDME experiments using the Fe^{3+}-containing protein cytochrome P450cam (CYP101) spin labeled at position C58 as a test case (Figure 1a). In addition, several methods for the suppression of ESEEM artifacts in the RIDME time trace are compared to each other.

MATERIALS AND METHODS

Cloning, Protein Expression, Purification, and Spin Labeling. The cytochrome P450cam gene from *Pseudomonas putida* was obtained via the Addgene repository in form of the pUS200 plasmid (https://www.addgene.org/17788/). The gene was PCR amplified using the following primers:

P450cam_fwd	TAATAACCATGGGGATGACGACTGAAACCATAC
P450cam_rev	TAATAACTCGAGTTATACCGCTTTGGTAGTCGC

The PCR product was digested with NcoI and XhoI and cloned into the pEHisTEV vector (Huanting Liu, University of St Andrews, U.K.). Native cysteines except C58 were removed by PCR techniques[37,38] using the following oligos:

C85S_fwd	GCGAGAGCCCGTTCATCCCTCGTGAAGCCG
C85S_rev	AACGGGCTCTCGCTGGAAAAGTGGCGGTAATCT
C136S_fwd	GCCAGCTCGCTGATCGAGAGCCTGCGCCCG
C136S_rev	GATCAGCGAGCTGGCCAGCTCCTGGATCCGGTT
C285S_fwd	CCGCTAGCGAGGAACTACTCCGGCGCTTCT
C285S_rev	TCCTCGCTAGCGGCTGGAATACGCTCGGGA
C334A_fwd	ACGCCGCTCCGATGCACGTCGACTTCAGTC
C334A_rev	ATCGGAGCGGCGTTTTCGCGCTCATCCAGG

In this way, the native cysteine at position 58 could be used for the spin labeling experiments. To express the protein, the plasmid was transformed into *Escherichia coli* C43 cells. The cells were grown at 37 °C in LB medium, supplemented with 50 μg/L kanamycin until an OD of 0.5 was reached. The cultures were then induced with 0.4 mM IPTG. Further, 2 mM 5-aminoleuvinic acid was added to increase the heme incorporation efficiency. After induction, the cells were incubated at 25 °C with shaking at 200 rpm and the expression was allowed to proceed overnight. After expression, the cells were harvested, resuspended in buffer A (50 mM sodium phosphate pH 6.0, 50 mM NaCl), and lysed using a constant systems cell disruptor. Cell debris and insoluble proteins were removed by centrifuging the lysate at 20 000 rpm for 20 min at 4 °C. The soluble fraction was loaded onto a 5 mL HisTrap Ni FF column (GE Healthcare), and the target protein was eluted using a gradient from 0 to 100% buffer B (50 mM sodium phosphate pH 6.0, 50 mM NaCl, 1 M imidazole). Peak fractions were pooled and dialyzed against buffer C (50 mM Tris pH 7.4, 300 mM NaCl) for 3 h at 4 °C before addition of 4 mg of TEV protease overnight at 4 °C. On the next day, the protease and uncleaved protein were removed by passing the sample through a 5 mL HisTrap Ni FF column. The flowthrough was concentrated using a Vivaspin 20 10.000 MWCO concentrator and loaded onto a Superdex 200 16/60 column (GE Healthcare). For labeling, a 5-fold excess of (1-oxyl-2,2,5,5-tetramethylpyrroline-3-methyl)-methanethiosulfonate (MTSSL) was added to the protein before incubation on ice for 3 h. Unbound label was later removed by means of a PD-10 column using either H_2O-based buffer (50 mM TES pH 7.4, 400 mM KCl) or D_2O-based buffer (50 mM TES pH 7.4, 400 mM KCl). Two samples obtained by this procedure were denoted in accordance to their buffer as C58R$_1$-H_2O and C58R$_1$-D_2O. For cryoprotection, 50% v/v ethylene glycol was added to C58R$_1$-H_2O and the same amount of deuterated ethylene glycol was added to C58R$_1$-D_2O. The final protein concentration in both samples was 150−200 μM.

EPR Measurements. All EPR measurements were carried out on a Bruker ELEXSYS E580 spectrometer. A Flexline probehead housing either an X-band (Bruker, ER 4118X-MD-5W1) or Q-band (Bruker, EN 5107D2) resonator was used. At the X-band all microwave pulses were amplified via a 1 kW TWT amplifier (Applied Systems Engineering, 117X). A standard Bruker 3W amplifier was used at the Q-band. To obtain low temperatures, a continuous flow helium cryostat (Oxford Instruments, CF935) and a temperature control system (Oxford Instruments, ITC 503S) were employed.

PELDOR experiments were performed with the standard four-pulse sequence shown in Figure 1b. The frequency of the pump pulse (ν_B) and the magnetic field were adjusted to excite the spins corresponding to the maximum of the nitroxide spectrum. The frequency of the detection pulses (ν_A) was set 250 MHz lower than the pump frequency, exciting a part of the

DOI: 10.1021/acs.jpcb.5b02118
J. Phys. Chem. B XXXX, XXX, XXX−XXX

Fe^{3+} spins. The $\pi/2$ and π pulses of the detection sequence had lengths of 16 and 32 ns, and the pump pulse was 18 ns long. The $\pi/2$ pulse was phase-cycled to eliminate receiver offsets. The τ_1 and τ_2 intervals were set to 360 ns and 1.3 μs, respectively, which allowed one to acquire 90 data points with a 16 ns time increment. The PELDOR signal was recorded at 10 K with a repetition time of 1 ms. To achieve an acceptable SNR, the signal was acquired for 24 h.

RIDME experiments were performed with the five-pulse sequence shown in Figure 1c. Before setting up the pulse sequence, the value of the magnetic field was adjusted to set the frequency of the microwave pulses in resonance with the maximum of the nitroxide spectrum. Depending on the protein buffer and frequency band, different lengths of the pulses and interpulse intervals were used; all their values are listed in Table 1. To eliminate the contribution of unwanted echoes, an eight-step phase cycling[26] was applied. The time increment for the displacement of the third and fourth pulses, defining the time resolution of the RIDME signals, was 16 ns. Totals of 100 and 156 data points were acquired for the $C58R_1$ in H_2O and $C58R_1$ in D_2O samples, respectively. All experiments were performed at 25 K with a repetition time of 10 ms and 1000 averages per data point resulting in an overall measurement time of ~2.3 h for $C58R_1$-H_2O and ~3.5 h for $C58R_1$-D_2O.

Table 1. Parameters of the RIDME Experiments on the $C58R_1$ Samples

sample	microwave frequency (GHz)	$t_{\pi/2}$, t_π (ns)	τ_1 (ns)	τ_2 (μs)	T (μs)
$C58R_1$-H_2O	9.720	16, 32	140	1.6	30
$C58R_1$-H_2O	9.720	80, 160	246	1.6	30
$C58R_1$-H_2O	33.760	24, 48	140	1.6	30
$C58R_1$-D_2O	33.738	24, 48	140	2.5	30
$C58R_1$-D_2O	33.736	120, 240	340	2.7	30

The distance distributions were extracted from the RIDME and PELDOR time traces by means of the program DeerAnalysis[39] using a regularization parameter of 1. A second-order polynomial was empirically chosen as a background function and fitted for both PELDOR and RIDME time traces.

RESULTS AND DISCUSSION

Characterization of Samples. Prior to the distance measurements, the synthesized $C58R_1$ samples were characterized with respect to the protein identity and purity, the degree of spin labeling, flexibility of the spin label, the spin state and the content of Fe^{3+} ions. According to the typical reddish color, circular dichroism (CD) spectroscopy, and gel chromatography, the mutant does have the expected structure and is pure (Figure S1, Supporting Information). On the basis of the continuous wave (cw) X-band EPR spectra recorded at 293 K (Figure S2, Supporting Information), the labeling degree is estimated to be higher than 80%. The cw EPR spectra also reveal that the protein-bound labels are significantly immobilized and adopt at least two distinct conformations (Supporting Information). The low-temperature cw EPR spectra showed the typical low-spin heme signal for cytochrome P450cam with the g-tensor (g_1, g_2, g_3) = (2.42, 2.25, 1.91) and no traces of the high-spin heme.[40] Using UV–vis spectroscopy, the ratio of heme per cytochrome molecule was roughly estimated to be 52% for the $C58R_1$-H_2O sample and 40% for the $C58R_1$-D_2O sample (Figure S3, Supporting Information). Note that the difference between the two samples is related to the fact that both samples were synthesized independently from each other.

Setting Up the Distance Measurements. Before performing the PELDOR and RIDME measurements on the Fe^{3+}-nitroxide spin pair one has to choose which spin will be used for recording the echo signal (referred to as spin A) and which spin will be flipped (referred to as spin B). The criteria of this assignment are different for PELDOR and RIDME. An efficient RIDME experiment requires the spin–lattice relaxation time of spin B to be much shorter than that of spin A.[24] This requirement is fulfilled, when spin A corresponds to a nitroxide and spin B is the faster relaxing Fe^{3+} center. In contrast, the use of the nitroxide as spin B is preferable for the PELDOR experiment, because this yields the larger modulation depth. Then, spin A will correspond to a subset of Fe^{3+} spins. Note that only those Fe^{3+} spins that have g-values close to g_3 could be used as spin A here, because the spectral separation between the nitroxide signal and the low-field part of the Fe^{3+} signal is much larger than the resonator bandwidth. The spectral positions of the microwave pulses are indicated in Figure 2 for the PELDOR and the RIDME setup.

PELDOR Measurements. As mentioned above, the PELDOR signal was acquired on the high-field region of the

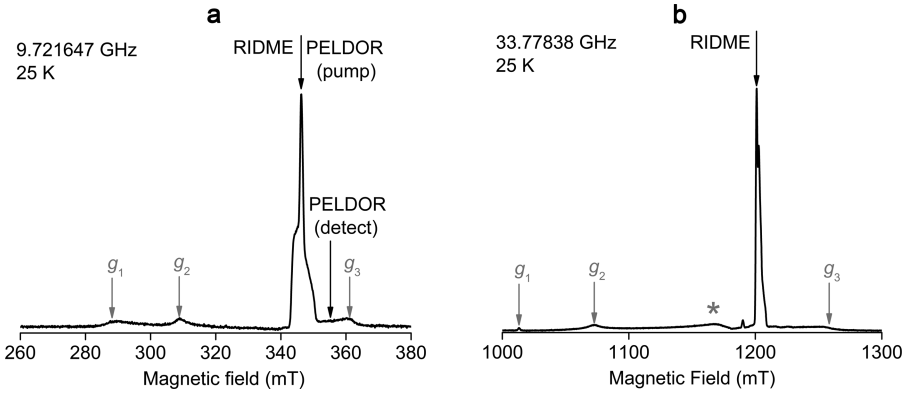

Figure 2. Field-swept echo-detected spectrum of $C58R_1$-H_2O recorded at (a) the X-band and (b) the Q-band. The components of the Fe^{3+} effective g-factors are shown by gray arrows. The spectral positions of the microwave pulses are indicated by black arrows. The signal in the Q-band spectrum marked by an asterisk corresponds to the copper background of the resonator.

DOI: 10.1021/acs.jpcb.5b02118
J. Phys. Chem. B XXXX, XXX, XXX–XXX

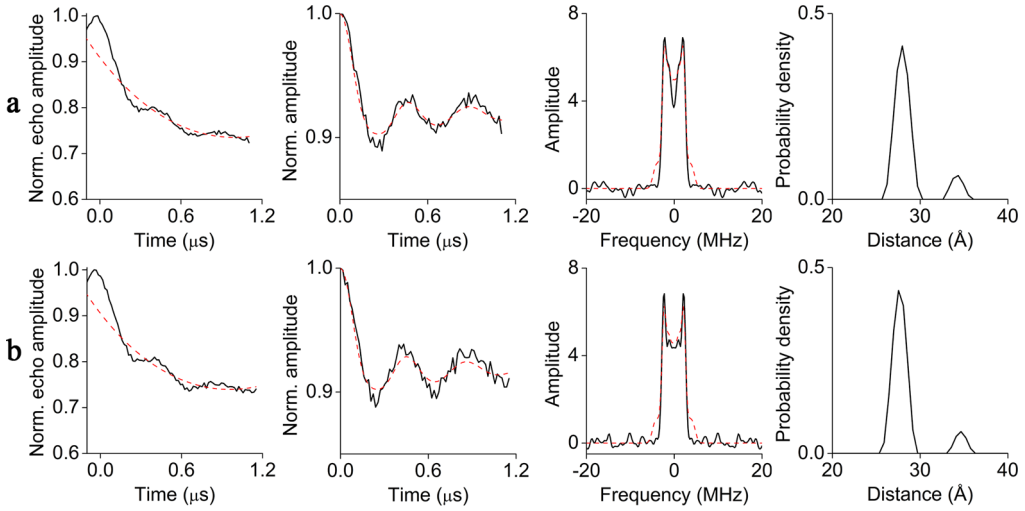

Figure 3. PELDOR data of (a) C58R$_1$-H$_2$O and (b) C58R$_1$-D$_2$O samples. Column 1: primary time traces (black lines) and their background fits (red dashed line). Column 2: background-subtracted time traces (black lines) and their fits by DeerAnalysis (red dashed lines). Column 3: FFT of the background-subtracted time traces and their fits by DeerAnalysis (red dashed lines). Column 4: derived Fe^{3+}-MTSSL distance distributions.

Fe^{3+} spectrum, whereas the nitroxide spins were flipped by the pump pulse. Because the phase memory time (T_m) of the Fe^{3+} ions in the C58R$_1$-H$_2$O and C58R$_1$-D$_2$O samples were found to be nearly the same (Figure S4, Supporting Information), the same interpulse intervals were used for both samples in the PELDOR experiments. The PELDOR time traces of both samples look identical (Figure 3). They have a modulation depth of 8% and comprise two periods of the dipolar modulation. The reasons for this weak modulation depth are incomplete labeling and orientation selectivity, which occurs because the detection pulses excite only a small fraction of the Fe^{3+} spectrum. The evidence of orientation selectivity can be clearly seen in the fast Fourier transform (FFT) of the time traces, which do not reproduce the shape of the Pake doublet (Figure 3). In the presence of orientation selectivity the extraction of distances by the program DeerAnalysis is not reliable anymore. For the accurate analysis of orientation selective PELDOR data, several time traces recorded on different spectral components of anisotropic spin centers are required.[41−43] This requirement could not be fulfilled here, because the separation between the nitroxide spectrum and the low-field components of the Fe^{3+} spectrum (g_1 and g_2 in Figure 2) is much larger than the resonator bandwidth and even the available frequency range of a commercial X-band spectrometer. Nevertheless, for the sake of comparison with the RIDME results, the obtained PELDOR time trace was analyzed by DeerAnalysis (Figure 3). A relatively good fit to the time trace was achieved, yielding a distance distribution with a mean value of 27.7 Å and a standard deviation of 0.8 Å. The small distance peak appearing at 35 Å is attributed to incomplete background removal and orientation selectivity.

RIDME Measurements. The five-pulse sequence illustrated in Figure 1c was used to perform the RIDME experiment. The Fe^{3+} spins, which were chosen to be the B spins, have to flip by spontaneous relaxation during the time interval T of this sequence. Thus, the value of T should be adjusted so that the majority of the Fe^{3+} spins are flipped. Because the relaxation rate of the Fe^{3+} spins is temperature dependent, the adjustment of T should be done together with the temperature adjustment to ensure the following additional requirements: T should not be too long, to minimize spectral diffusion effects, but still much longer than the maximal interval t, so that the spin−lattice relaxation of the Fe^{3+} spin during t can be neglected.[24] To determine T experimentally, a series of inversion recovery curves were recorded on the C58R$_1$-H$_2$O sample at different temperatures (Figure 4). A T value of 30 μs, which corresponds

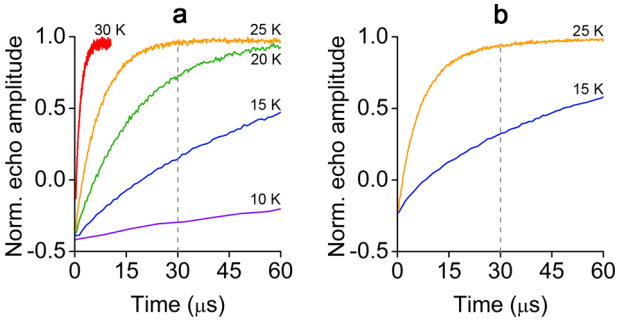

Figure 4. Inversion recovery for the Fe^{3+} spin center in C58R$_1$-H$_2$O recorded at different temperatures and at (a) the X-band and (b) the Q-band. The dashed line corresponds to the T value chosen for RIDME.

to almost complete recovery of the Fe^{3+} longitudinal magnetization at 25 K and, therefore, to the highest probability of the Fe^{3+} spin flip at this temperature, was chosen for the RIDME measurements.[29] Note that the chosen values of T and temperature provide a good compromise between the requirements mentioned above (Figures S5 and S6, Supporting Information).

The X-band RIDME time trace recorded on the C58R$_1$-H$_2$O sample is shown in Figure 5a. The FFT of this signal consists of the Pake pattern appearing at frequencies <5 MHz and a peak around 14.7 MHz corresponding to the ^{1}H Larmor frequency (Figure 5b). Although the dipolar and ESEEM frequencies are well separated from each other, it is worthwhile to get rid of the proton ESEEM for the simplicity of the further RIDME data analysis. To do this, four different approaches were considered.

As proposed in previous works,[29,30] ESEEM can be suppressed through dividing an original RIDME signal by a reference RIDME signal which contains ESEEM, but no dipolar modulation. Such a reference signal is obtained, when the

DOI: 10.1021/acs.jpcb.5b02118
J. Phys. Chem. B XXXX, XXX, XXX−XXX

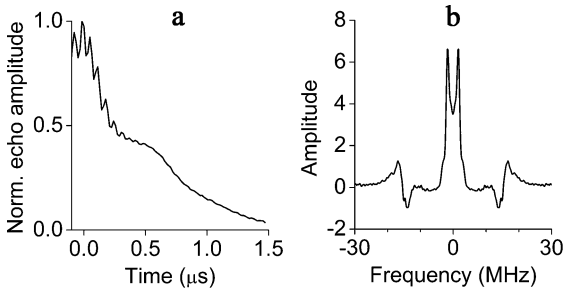

Figure 5. (a) RIDME time trace acquired on C58R$_1$-H$_2$O at the X-band and (b) its FFT.

inversion of the Fe^{3+} spins during the time interval T is made inefficient. The conditions leading to inefficient inversion are readily determined from Figure 4: either the T interval should be shortened, i.e., from 30 μs down to 2 μs, or the temperature of the experiment should be lowered, i.e., from 25 K down to 15 K. Both conditions were applied here to record the reference RIDME signal, which was then used to normalize the original RIDME signal. The resulting normalized time traces are compiled in Figure 6a,b. They reveal that the normalization via temperature allows one to remove ESEEM completely, whereas after the normalization via T some ESEEM artifacts are still present in the data.

Another possibility to suppress ESEEM is to use selective microwave pulses. Note that the RIDME signal described above was acquired with rather broadband $\pi/2$ and π pulses of 16 and 32 ns, respectively. Because the excitation bandwidths corresponding to these pulses (37.5 and 18.7 MHz) are larger than the ^{1}H Larmor frequency, proton ESEEM contributes to the signal. However, when the excitation bandwidth of the microwave pulses is much smaller than the ^{1}H Larmor frequency, it can be suppressed.[31] The RIDME signal acquired on the C58R$_1$-H$_2$O sample with 80 and 160 ns pulses is shown in Figure 6c. As can be seen, the signal contains the dipolar modulation and, importantly, no traces of proton ESEEM. Besides, this approach does not require the acquisition of a reference time trace reducing the measurement time by a factor

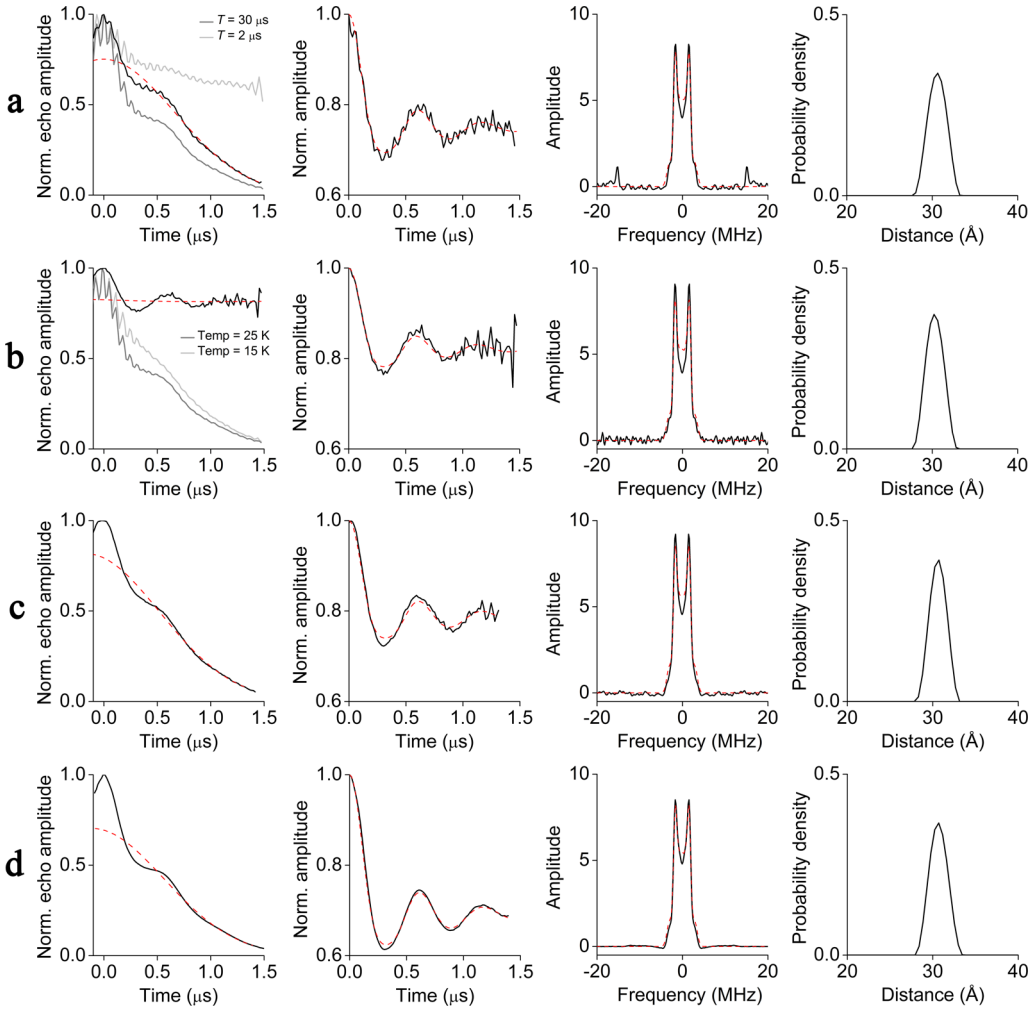

Figure 6. Different approaches of ESEEM removal from the RIDME signal acquired on C58R$_1$-H$_2$O: (a) ESEEM is removed by division of two RIDME signals recorded with T = 30 μs and T = 2 μs. The division result is shown as a black line. (b) ESEEM is removed by division of two RIDME signals recorded at 25 and 15 K. The division result is shown as a black line. (c) ESEEM is suppressed by using selective pulses with lengths of 80 and 160 ns for π and $\pi/2$ pulses, respectively. (d) ESEEM is suppressed by performing RIDME at Q-band frequencies. Column 1: primary time traces (black lines) and their background fits (red dashed lines). Column 2: background-subtracted time traces (black lines) and their fits by DeerAnalysis (red dashed lines). Column 3: FFT of the background-subtracted time traces and their fits by DeerAnalysis (red dashed lines). Column 4: derived Fe^{3+}-MTSSL distance distributions.

DOI: 10.1021/acs.jpcb.5b02118
J. Phys. Chem. B XXXX, XXX, XXX−XXX

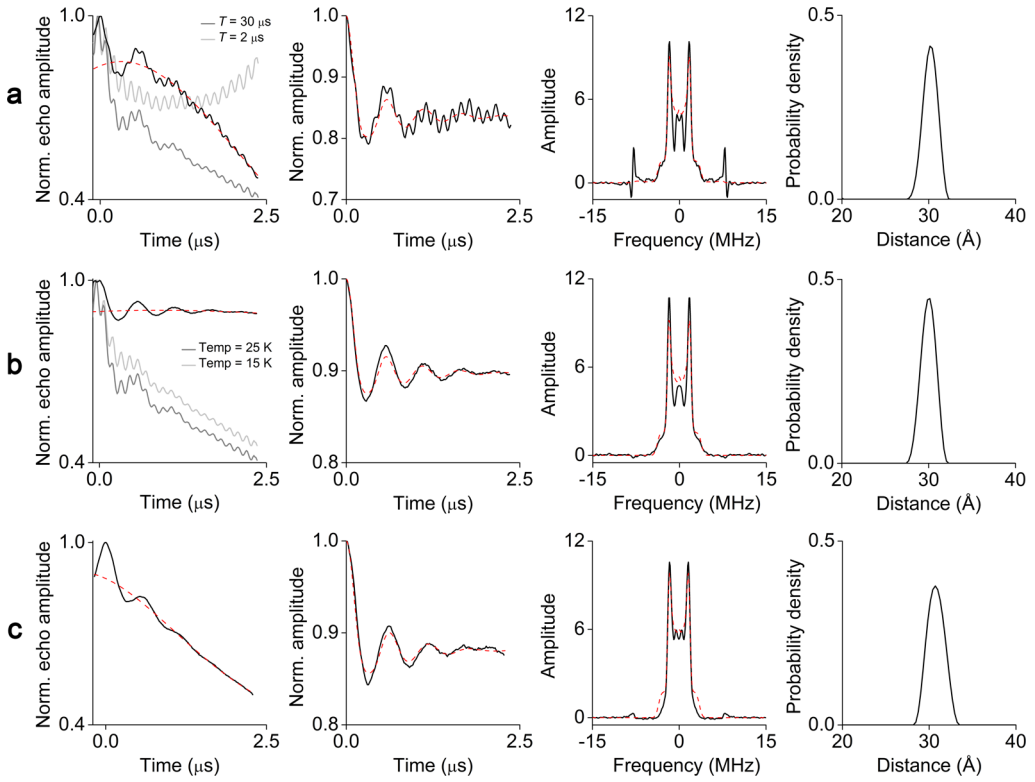

Figure 7. Different approaches of ESEEM removal from the Q-band RIDME signal acquired on C58R$_1$-D$_2$O. (a) ESEEM is removed by division of two RIDME signals recorded with T = 30 μs and T = 2 μs. The division result is shown by black line. (b) ESEEM is removed by division of two RIDME signals recorded at 25 and 15 K. The division result is shown by black line. (c) ESEEM is suppressed by using 120 and 240 ns pulses. Column 1: primary time traces (black lines) and their background fits (gray dashed lines). Column 2: background-subtracted time traces (black lines) and their fits by DeerAnalysis (gray dashed lines). Column 3: FFT of the background-subtracted time traces and their fits by DeerAnalysis (gray dashed lines). Column 4: derived Fe^{3+}-MTSSL distance distributions.

of 2. The same also implies the use of high microwave frequencies, which reduce the probability of forbidden transitions and, consequently, the amplitude of ESEEM.[34] Moreover, because the ^{1}H Larmor frequency increases proportionally with the microwave frequency/magnetic field ($\nu_I(^1H)$ = 51.1 MHz at 1.2 T), the condition when the excitation bandwidth of the microwave pulses is much smaller than the ^{1}H Larmor frequency can be achieved without significant elongation of the pulses. The RIDME signal recorded at the Q-band confirms the efficiency of this approach (Figure 6d).

The conversion of the RIDME time traces into distance distributions was done by means of the program DeerAnalysis. First, a decay with an empirically chosen shape of second-order polynomial was removed from the time traces (Figure 6, column 1). As mentioned in previous work,[33] a theoretical description of the RIDME background is still absent, but one important contribution to it is probably spin diffusion caused by interactions of the nitroxide spin with surrounding magnetic nuclei.[26] However, because the time traces exhibit a prominent modulation, the influence of the background function on the subsequently derived distances is expected to be negligible. The background-corrected time traces feature modulation depths of 18−30% (Figure 6, column 2). This variation of the modulation depth may be caused by differences in the ESEEM suppression procedures and the error of the background fitting. Note that the division of the two time traces used to remove the ESEEM reduces the contribution of the background to the RIDME signals but does not eliminate it completely (Figure 6a,b). The obtained modulation depths are lower than the theoretically achievable value of 50%,[26] which is attributed to the fraction of cytochrome molecules containing no heme group as described above and to free nitroxides. In principle, the low modulation depth could also stem from a nonoptimal value for T. However, this possibility was excluded by recording the dependence of the modulation depth parameter on T (Figure S5, Supporting Information). The time traces corresponding to different procedures of ESEEM suppression have also slightly different SNRs. The lowest average SNR corresponds to the procedures using a reference time trace. This is probably due to the division of two low-amplitude signals at high t values. The time trace recorded with selective pulses might have been expected to show the lowest SNR, because fewer spins are excited, but because it does not require the division by a reference signal, it actually has a SNR that is ∼5 times higher. Also the Q-band time trace has a gain in SNR of ∼68 compared to the reference procedures at the X-band. FFT of the time traces yield the characteristic Pake doublet, meaning that the RIDME experiment recorded on the maximum of the nitroxide spectrum has apparently no orientation selectivity (Figure 6, column 3). In contrast, recording the RIDME experiment at other positions on the nitroxide spectrum shows that orientation selection can be introduced into RIDME if wanted (Figure S7, Supporting Information). Finally, the time traces were transformed into a distance distributions using Tikhonov regularization. A good fit was obtained for the distance distribution with a mean value of 30.5 Å and a standard deviation of 1.0 Å. Significantly, the distance distributions are invariant with respect to the different

DOI: 10.1021/acs.jpcb.5b02118
J. Phys. Chem. B XXXX, XXX, XXX−XXX

ESEEM suppression procedures (Figure S8, Supporting Information).

Due to the limited T_m of the nitroxide spins, the RIDME signals decay to zero after roughly 1.5 μs (Figure 6). Nevertheless, this time window allows the robust determination of distances up to 45 Å.[2] To increase this limit, T_m of the nitroxide spins was prolonged by using deuterated buffer for the C58R$_1$-D$_2$O sample.[44] Note that the ^{2}D Larmor frequency is similar to the observed dipolar frequencies at the X-band ($\nu_I(^2D)$ = 2.29 MHz at 350 mT) and bigger than these frequencies at the Q-band ($\nu_I(^2D)$ = 7.85 MHz at 1.2 T). Therefore, to avoid the complexity related to the deuterium ESEEM removal at the X-band, the RIDME experiments were performed at the Q-band. Running the Q-band RIDME experiment with the same pulse lengths as for the C58R$_1$-H$_2$O sample (24/48 ns) yielded time traces that still contain a considerable ESEEM contribution (Figure 7a,b). Thus, to eliminate the ESEEM artifacts, the Q-band RIDME signal was normalized with a reference signal. Similar to the C58R$_1$-H$_2$O sample, normalization of the RIDME time trace via temperature is more efficient than normalization via T.

In the following, the time trace obtained after normalization via temperature is discussed exemplarily (Figure 7b). Due to the deuterated buffer, a nonzero echo signal is detected even after 2.5 μs, which allows observing more than two well-resolved periods of the dipolar modulation. However, the obtained modulation depth of 10% is lower than the modulation depths observed for the C58R$_1$-H$_2$O sample. This is attributed to the lower heme content in the C58R$_1$-D$_2$O (40%) as compared to the C58R$_1$-H$_2$O (52%) sample. The distance distribution obtained from this time trace yields a mean distance of 30.1 Å and a standard deviation of 0.8 Å, which is in agreement with the distances found for C58R$_1$-H$_2$O.

The use of selective 120 and 240 ns pulses not only led to nearly complete suppression of ESEEM but also caused the loss of the high-frequency component of the Pake pattern (Figure 7c). The lack of this component may either be due to orientation selectivity resulting from the selective excitation of nitroxide spins by the long microwave pulses or may be due to the suppression of the largest dipolar frequencies by the microwave pulses in the same way as they suppress ESEEM. The second assumption is supported by the fact that the excitation bandwidth corresponding to 240 ns π-pulse (2.5 MHz) is lower than the missing frequencies of the Pake doublet.

Comparison of the PELDOR and RIDME Results. Measurements of Fe^{3+}−MTSSL distances conducted on the C58R$_1$ samples reveal several advantages of RIDME over PELDOR. First of all, the RIDME experiment allows obtaining the whole dipolar spectrum (Pake doublet), whereas some dipolar frequencies are absent in the PELDOR-derived spectrum due to orientation selectivity. This makes the analysis of RIDME data easier and the corresponding distance distribution more reliable.

Second, the RIDME time traces have better SNR and therefore require shorter measurement time as compared to the PELDOR time trace. The X-band RIDME signal (Figure 6c) acquired on the C58R$_1$-H$_2$O sample has a 7 times higher SNR as compared to the corresponding X-band PELDOR signal (Figure 3a). In addition, to account for orientation selectivity in PELDOR data analysis, several time traces at different orientations would have to be recorded that would increase the measurement time, thus favoring the RIDME experiment even more. Recording the PELDOR time traces at the Q-band with a 150 W TWT amplifier may increase SNR by a factor of 13−20,[45] but a similar increase in SNR is then expected also for the RIDME time trace (Figure 6c,d). Moreover, increased orientation selectivity is expected for Q-band PELDOR time traces, because the Fe^{3+} spectrum is g-dominated and therefore broader at Q-band than at X-band.

Importantly, the use of deuterated buffer allowed one to increase the length of the RIDME time trace up to 2.5 μs. At the same time, the length of the PELDOR time trace reaches 1.5 μs only, because the signal is recorded on the fast relaxing Fe^{3+} centers. In principle, the PELDOR time trace could be recorded on the slower relaxing nitroxide spin, while flipping the Fe^{3+} spins. However, this would lead to a small modulation depth, due to the small part of the Fe^{3+} spins flipped by the pump pulse, and longer shot repetition time, because of the slower longitudinal relaxation of the nitroxide.

The modulation depths of the PELDOR and RIDME time traces are with ∼10% similar for the C58R$_1$-D$_2$O sample and differ by 10−15% for the C58R$_1$-H$_2$O sample. Note that each method has its own specific factors influencing the value of the modulation depth. As mentioned above, the RIDME modulation depth is affected by the heme content in the samples. At the same time, the PELDOR modulation depth is dependent here on the labeling degree and orientation selection.

Both methods require the suppression of ESEEM artifacts in their time traces. In PELDOR data these artifacts are weak and can be suppressed by recording time traces for the several τ values. In contrast, the RIDME experiment can have considerable ESEEM contributions in the time trace. Nevertheless, four different ways of ESEEM removal applied for RIDME have been shown to be efficient and easy to implement.

The distance distributions obtained by PELDOR and RIDME are overlaid in Figure 8. The corresponding mean

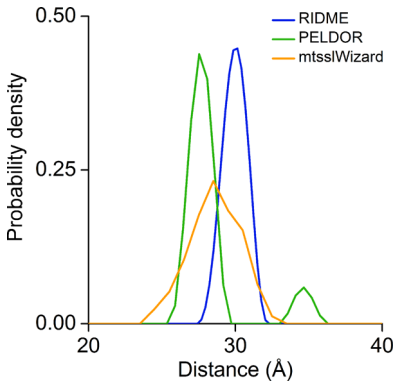

Figure 8. Comparison of the experimental and simulated Fe^{3+}-MTSSL distances in the mutant C58R$_1$.

distances differ by 2.4 Å. This difference is mainly attributed to the error of the PELDOR-derived distance, which stems from the inexact analysis of orientation selective PELDOR data as well as from the short length of the PELDOR time trace. Because of the same reasons, the similarity of the distribution widths is considered as accidental. Nevertheless, both experimental distributions fit to the prediction, obtained from molecular modeling by the program mtsslWizard[35,36] and using the crystal structure of cytochrome P450cam (PDB 3L61). In

DOI: 10.1021/acs.jpcb.5b02118
J. Phys. Chem. B XXXX, XXX, XXX−XXX

addition, the narrow distance distribution observed by RIDME can be correlated to the significantly reduced flexibility of the label revealed by the cw X-band EPR spectra (see above).

CONCLUSION

The five-pulse RIDME experiment has been shown to be more suitable than PELDOR for the distance measurements between the Fe^{3+} ion and nitroxide spin label. The main advantages of the RIDME experiment are that it is less affected by orientation selectivity, which can even be avoided in the present case, and that the SNR is 7 times higher. This, in turn, allows for an easy and robust conversion of the RIDME signals into distance distributions. The use of deuterated protein buffer was shown to provide a longer RIDME signal but may, for the sake of separating dipolar frequencies from ESEEM artifacts, require the use of microwave frequencies higher than X-band.

Four different methods of ESEEM suppression in the RIDME signal were tested. The method in which the original signal is normalized by the reference signal recorded at lower temperature was shown to be more efficient than the one in which the reference signal was obtained by varying the T interval. The use of Q-band frequency allowed the suppression of proton ESEEM but was not high enough to suppress deuterium ESEEM. As an alternative method, the use of long selective microwave pulses was successfully applied. However, it requires the dipolar frequencies to be lower than the ESEEM frequencies that will be not always fulfilled for short distances at particular microwave frequency. Importantly, we have shown that none of these methods for ESEEM removal affected the final distance distribution. Thus, five-pulse RIDME holds great promise for distance measurements to metal centers. In addition, it was shown recently that five-pulse RIDME can be applied to high-spin metal ions although higher harmonics of the dipolar coupling constant have to be taken into account.[33]

Notably, the use of arbitrary waveform broadband microwave pulses may improve the performance of PELDOR measurements for the Fe^{3+}−nitroxide spin pairs with respect to SNR, orientation selectivity and modulation depth as recently shown for bisnitroxides.[46] If one can excite the whole nitroxide spectrum with the broadband pulses, RIDME measurements on given spin system may also get advantage from using such pulses.

ASSOCIATED CONTENT

Supporting Information

The SDS-PAGE analysis, size-exclusion chromatogram, CD spectra, cw EPR spectra, UV−vis spectra, 2-pulse ESEEM of the cytochrome P450cam mutant C58R_1. The Supporting Information is available free of charge on the ACS Publications website at DOI: 10.1021/acs.jpcb.5b02118.

AUTHOR INFORMATION

Corresponding Author

*O. Schiemann. E-mail: schiemann@pc.uni-bonn.de. Phone: +49(0)228-732989.

Notes

The authors declare no competing financial interest.

ACKNOWLEDGMENTS

We gratefully acknowledge financial support of the Deutsche Forschungsgemeinschaft through the Collaborative Research Center SFB813 “Chemistry at Spin Centers”. We also thank Prof. Arne Lützen and Christina Tenten (University of Bonn) for assistance with CD measurements.

REFERENCES

(1) Schiemann, O.; Prisner, T. F. Long-Range Distance Determinations in Biomacromolecules by EPR Spectroscopy. *Q. Rev. Biophys.* **2007**, *40*, 1−53.

(2) Jeschke, G. DEER Distance Measurements on Proteins. *Annu. Rev. Phys. Chem.* **2012**, *63*, 419−446.

(3) Borbat, P. P.; Freed, J. H. Pulse Dipolar Electron Spin Resonance: Distance Measurements. In *Structure and Bonding (Berlin)*; Timmel, C. R., Harmer, J., Eds.; Springer: Heidelberg, 2013; Vol. *152*, pp 206−210, pp 1−82.

(4) Milov, A. D.; Salikhov, K. M.; Shirov, M. D. Application of ELDOR in Electron-Spin Echo for Paramagnetic Center Space Distribution in Solids. *Fiz. Tverd. Tela* **1981**, *23*, 975−982.

(5) Martin, R. E.; Pannier, M.; Diederich, F.; Gramlich, V.; Hubrich, M.; Spiess, H. W. Determination of End-to-End Distances in a Series of TEMPO Diradicals of up to 2.8 nm Length with a New Four-Pulse Double Electron Electron Resonance Experiment. *Angew. Chem., Int. Ed.* **1998**, *37*, 2833−2837.

(6) van Amsterdam, I. M. C.; Ubbink, M.; Canters, G. W.; Huber, M. Measurement of a Cu-Cu Distance of 26 Å by a Pulsed EPR Method. *Angew. Chem., Int. Ed.* **2003**, *42*, 62−64.

(7) Kay, C. W. M.; El Mkami, H.; Cammack, R.; Evans, R. W. Pulsed ELDOR Determination of the Intramolecular Distance between the Metal Binding Sites in Dicupric Human Serum Transferrin and Lactoferrin. *J. Am. Chem. Soc.* **2007**, *129*, 4868−4869.

(8) Yang, Z.; Kurpiewski, M. R.; Ji, M.; Townsend, J. E.; Mehta, P.; Jen-Jacobson, L.; Saxena, S. ESR Spectroscopy Identifies Inhibitory Cu^{2+} Sites in a DNA-Modifying Enzyme to Reveal Determinants of Catalytic Specificity. *Proc. Natl. Acad. Sci. U.S.A.* **2012**, *109*, E993−E1000.

(9) Denysenkov, V. P.; Prisner, T. F.; Stubbe, J.; Bennati, M. High-Field Pulsed Electron-Electron Double Resonance Spectroscopy to Determine the Orientation of the Tyrosyl Radicals in Ribonucleotide Reductase. *Proc. Natl. Acad. Sci. U.S.A.* **2006**, *103*, 13386.

(10) Denysenkov, V. P.; Biglino, D.; Lubitz, W.; Prisner, T. F.; Bennati, M. Structure of the Tyrosyl Biradical in Mouse R2 Ribonucleotide Reductase from High-Field PELDOR. *Angew. Chem., Int. Ed.* **2008**, *47*, 1224−1227.

(11) Kay, C. W. M.; Elsässer, C.; Bittl, R.; Farrell, S. R.; Thorpe, C. Determination of the Distance between the Two Neutral Flavin Radicals in Augmenter of Liver Regeneration by Pulsed ELDOR. *J. Am. Chem. Soc.* **2006**, *128*, 76−77.

(12) Swanson, M. A.; Kathirvelu, V.; Majtan, T.; Frerman, F. E.; Eaton, G. R.; Eaton, S. S. DEER Distance Measurement Between a Spin Label and a Native FAD Semiquinone in Electron Transfer Flavoprotein. *J. Am. Chem. Soc.* **2009**, *131*, 15978−15979.

(13) Abdullin, D.; Florin, N.; Hagelueken, G.; Schiemann, O. EPR-Based Approach for the Localization of Paramagnetic Metal Ions in Biomolecules. *Angew. Chem., Int. Ed.* **2015**, *54*, 1827−1831.

(14) Elsässer, C.; Brecht, M.; Bittl, R. Pulsed Electron-Electron Double Resonance on Multinuclear Metal Clusters: Assignment of Spin Projection Factors Based on the Dipolar Interaction. *J. Am. Chem. Soc.* **2002**, *124*, 12606−12611.

(15) Roessler, M. M.; King, M. S.; Robinson, A. J.; Armstrong, F. A.; Harmer, J.; Hirst, J. Direct Assignment of EPR Spectra to Structurally Defined Iron-Sulfur Clusters in Complex I by Double Electron-Electron Resonance. *Proc. Natl. Acad. Sci. U.S.A.* **2010**, *107*, 1930−1935.

(16) Kawamori, A.; Katsuta, N.; Mino, H.; Ishii, A.; Minagawa, J.; Ono, T.-A. Positions of Q_A and Chl_Z Relative to Tyrosine Y_Z and Y_D in Photosystem II Studied by Pulsed EPR. *J. Biol. Phys.* **2002**, *28*, 413−426.

(17) Goldfarb, D. Gd^{3+} Spin Labeling for Distance Measurements by Pulse EPR Spectroscopy. *Phys. Chem. Chem. Phys.* **2014**, *16*, 9685−9699.

DOI: 10.1021/acs.jpcb.5b02118
J. Phys. Chem. B XXXX, XXX, XXX−XXX

(18) Yulikov, M. Spectroscopically Orthogonal Spin Labels and Distance Measurements in Biomolecules. *Electron Paramagn. Reson.* **2015**, *24*, 1−31.
(19) Ezhevskaya, M.; Bordignon, E.; Polyhach, Y.; Moens, L.; Dewilde, S.; Jeschke, G.; Van Doorslaer, S. Distance Determination between Low-Spin Ferric Haem and Nitroxide Spin Label Using DEER: the neuroglobin case. *Mol. Phys.* **2013**, *111*, 2855−2864.
(20) Banerjee, D.; Yagi, H.; Huber, T.; Otting, G.; Goldfarb, D. Nanometer-Range Distance Measurement in a Protein Using Mn^{2+} Tags. *J. Phys. Chem. Lett.* **2012**, *3*, 157−160.
(21) Akhmetzyanov, D.; Plackmeyer, J.; Endeward, B.; Denysenkov, V.; Prisner, T. F. Pulsed Electron-Electron Double Resonance Spectroscopy between a High-Spin Mn^{2+} Ion and a Nitroxide Spin Label. *Phys. Chem. Chem. Phys.* **2015**, *17*, 6760−6766.
(22) Kaminker, I.; Bye, M.; Mendelman, N.; Gislason, K.; Sigurdsson, S. Th.; Goldfarb, D. Distance Measurements between Manganese(II) and Nitroxide Spin-Labels by DEER Determine a Binding Site of Mn^{2+} in the HP92 Loop of Ribosomal RNA. *Phys. Chem. Chem. Phys.* **2015**, DOI: 10.1039/C5CP01624J.
(23) Rakowsky, M. H.; More, K. M.; Kulikov, A. V.; Eaton, G. R.; Eaton, S. S. Time-Domain Electron Paramagnetic Resonance as a Probe of Electron-Electron Spin-Spin Interaction in Spin-Labeled Low-Spin Iron Porphyrins. *J. Am. Chem. Soc.* **1995**, *117*, 2049−2057.
(24) Kulik, L. V.; Dzuba, S. A.; Grigoryev, I. A.; Tsvetkov, Y. D. Electron Dipole-Dipole Interaction in ESEEM of Nitroxide Biradicals. *Chem. Phys. Lett.* **2001**, *343*, 315−324.
(25) Kulik, L. V.; Grishin, Y. A.; Dzuba, S. A.; Grigoryev, I. A.; Klyatskaya, S. V.; Vasilevsky, S. F.; Tsvetkov, Y. D. Electron Dipole-Dipole ESEEM in Field-Step ELDOR of Nitroxide Biradicals. *J. Magn. Reson.* **2002**, *157*, 61−68.
(26) Milikisyants, S.; Scarpelli, F.; Finiguerra, M. G.; Ubbink, M.; Huber, M. A Pulsed EPR Method to Determine Distances between Paramagnetic Centers with Strong Spectral Anisotropy and Radicals: the Dead-Time Free RIDME Sequence. *J. Magn. Reson.* **2009**, *201*, 48−56.
(27) Savitsky, A.; Dubinskii, A. A.; Flores, M.; Lubitz, W.; Möbius, K. Orientation-Resolving Pulsed Electron Dipolar High-Field EPR Spectroscopy on Disordered Solids: I. Structure of Spin-Correlated Radical Pairs in Bacterial Photosynthetic Reaction Centers. *J. Phys. Chem. B* **2007**, *111*, 6245−6262.
(28) Bogachev, A. V.; Kulik, L. V.; Bloch, D. A.; Bertsova, Y. V.; Fadeeva, M. S.; Verkhovsky, M. I. Redox Properties of the Prosthetic Groups of Na^+-Translocating NADH:Quinone Oxidoreductase. 1. Electron Paramagnetic Resonance Study of the Enzyme. *Biochemistry* **2009**, *48*, 6291−6298.
(29) Astashkin, A. V.; Elmore, B. O.; Fan, W.; Guillemette, J. G.; Feng, C. Pulsed EPR Determination of Distance between Heme Iron and FMN Centers in a Human Inducible Nitric Oxide Synthase. *J. Am. Chem. Soc.* **2010**, *132*, 12059−12067.
(30) Savitsky, A.; Dubinskii, A. A.; Zimmermann, H.; Lubitz, W.; Möbius, K. High-Field Dipolar Electron Paramagnetic Resonance (EPR) Spectroscopy of Nitroxide Biradicals for Determining Three-Dimensional Structures of Biomacromolecules in Disordered Solids. *J. Phys. Chem. B* **2011**, *115*, 11950−11963.
(31) Astashkin, A. V.; Rajapakshe, A.; Cornelison, M. J.; Johnson-Winters, K.; Enemark, J. H. Determination of the Distance between the Mo(V) and Fe(III) Heme Centers of Wild Type Human Sulfite Oxidase by Pulsed EPR Spectroscopy. *J. Phys. Chem. B* **2012**, *116*, 1942−1950.
(32) Savitsky, A.; Niklas, J.; Golbeck, J. H.; Möbius, K.; Lubitz, W. Orientation Resolving Dipolar High-Field EPR Spectroscopy on Disordered Solids: II. Structure of Spin-Correlated Radical Pairs in Photosystem I. *J. Phys. Chem. B* **2013**, *117*, 11184−11199.
(33) Razzaghi, S.; Qi, M.; Nalepa, A. I.; Godt, A.; Jeschke, G.; Savitsky, A.; Yulikov, M. RIDME Spectroscopy with Gd(III) Centers. *J. Phys. Chem. Lett.* **2014**, *5*, 3970−3975.
(34) Schweiger, A.; Jeschke, G. *Principles of Pulse Electron Paramagnetic Resonance*; Oxford University Press: Oxford, U.K., 2001.
(35) Hagelüken, G.; Ward, R.; Naimsith, J. H.; Schiemann, O. MtsslWizard: In silico Spin-Labelling and Generation of Distance Distributions in PyMOL. *Appl. Magn. Reson.* **2012**, *42*, 377−391.
(36) Hagelueken, G.; Abdullin, D.; Ward, R.; Schiemann, O. In Silico Spin Labelling, Trilateration and Distance-Constrained Rigid Body Docking in PyMOL. *Mol. Phys.* **2013**, *111*, 2757−2766.
(37) Stoll, S.; Lee, Y.-T.; Zhang, M.; Wilson, R. F.; Britt, R. D.; Goodin, D. B. Double Electron-Electron Resonance Shows Cytochrome P450cam Undergoes a Conformational Change in Solution upon Binding Substrate. *Proc. Natl. Acad. Sci. U. S. A.* **2012**, *109*, 12888−12893.
(38) Liu, H.; Naismith, J. An Efficient One-Step Site-Directed Deletion, Insertion, Single and Multiple-Site Plasmid Mutagenesis Protocol. *BMC Biotechnol.* **2008**, 8−91.
(39) Jeschke, G.; Chechik, V.; Ionita, P.; Godt, A.; Zimmermann, H.; Banham, J.; Timmel, C. R.; Hilger, D.; Jung, H. DeerAnalysis2006 − a comprehensive software package for analyzing pulsed ELDOR data. *Appl. Magn. Reson.* **2006**, *30*, 473−498.
(40) Masuya, F.; Tsubaki, M.; Makino, R.; Hori, H. EPR Studies on the Photoproducts of Ferric Cytochrome P450cam (CYP101) Nitrosyl Complexes: Effects of Camphor and Its Analogues on Ligand-Bound Structures. *J. Biochem.* **1994**, *116*, 1146−1152.
(41) Narr, E.; Godt, A.; Jeschke, G. Selective Measurements of a Nitroxide-Nitroxide Separation of 5 nm and a Nitroxide-Copper Separation of 2.5 nm in a Terpyridine-Based Copper(II) Complex by Pulse EPR Spectroscopy. *Angew. Chem., Int. Ed.* **2002**, *41*, 3907−3910.
(42) Bode, B. E.; Plackmeyer, J.; Prisner, T. F.; Schiemann, O. PELDOR Measurements on a Nitroxide-Labeled Cu(II) Porphyrin: Orientation Selection, Spin-Density Distribution, and Conformational Flexibility. *J. Phys. Chem. A* **2008**, *112*, 5064−5073.
(43) Lovett, J. E.; Bowen, A. M.; Timmel, C. R.; Jones, M. W.; Dilworth, J. R.; Caprotti, D.; Bell, S. G.; Wong, L. L.; Harmer, J. Structural Information from Orientationally Selective DEER Spectroscopy. *Phys. Chem. Chem. Phys.* **2009**, *11*, 6840−6848.
(44) Lindgren, M.; Eaton, G. R.; Eaton, S. S.; Jonsson, B. H.; Hammarstrom, P.; Svensson, M.; Carlsson, U. Electron Spin Echo Decay as a Probe of Aminoxyl Environment in Spin-Labeled Mutants of Human Carbonic Anhydrase II. *J. Chem. Soc., Perkin Trans.* **1997**, *2*, 2549−2554.
(45) Polyhach, Y.; Bordignon, E.; Tschaggelar, R.; Gandra, S.; Godt, A.; Jeschke, G. High Sensitivity and Versatility of the DEER Experiment on Nitroxide Radical Pairs at Q-band Frequencies. *Phys. Chem. Chem. Phys.* **2012**, *14*, 10762−10773.
(46) Spindler, P. E.; Glaser, S. J.; Skinner, T. E.; Prisner, T. F. Broadband Inversion PELDOR Spectroscopy with Partially Adiabatic Shaped Pulses. *Angew. Chem., Int. Ed.* **2013**, *52*, 3425−3429.

DOI: 10.1021/acs.jpcb.5b02118
J. Phys. Chem. B XXXX, XXX, XXX−XXX